Measurement of the scalar Stark shift of the $6\,^1S_0 \rightarrow 6\,^3P_1$ transition in Hg

D. M. Harber and M. V. Romalis
Department of Physics, University of Washington, Seattle, Washington 98195
(Received 22 February 2000; published 28 November 2000)

The scalar Stark shift of the 254-nm intercombination $6\,^1S_0 \rightarrow 6\,^3P_1$ line in Hg was measured using a Doppler-shift frequency calibration technique. It is equal to -3.32 ± 0.06 kHz/(kV/cm)^2. This measurement can be used to test more accurate calculations of Hg atomic wave functions.

DOI: 10.1103/PhysRevA.63.013402 PACS number(s): 32.60.+i, 32.10.Dk, 32.80.Ys, 11.30.Er

I. INTRODUCTION

Precision measurements of the Stark shifts in alkali-metal atoms [1,2] have been used to refine the calculations of alkali-metal atomic wave functions, motivated, in part, by precision parity nonconservation measurements in Cs. Hg atoms are used to set one of the most significant limits on a permanent electric dipole moment (EDM) [3]. The search for an EDM does not require very precise atomic calculations, since any nonzero EDM would imply T and CP violation beyond the Standard Model. Nevertheless, recent calculations of CP-violating effects in ^{199}Hg [4] indicate that current atomic theory is one of the leading uncertainties in the interpretation of the ^{199}Hg EDM limit. The EDM of ^{199}Hg is due to the Schiff moment of the ^{199}Hg nucleus, which is produced by CP-violating nucleon-nucleon interactions and has been calculated using a nuclear shell model with an estimated accuracy of 50% [5]. Possible enhancements of the Schiff moment due to collective nuclear excitations have been considered recently [7], although no definite estimates exist. Atomic calculations, relating the Schiff moment to the EDM of ^{199}Hg atom, have been done using many-body perturbation theory with an estimated accuracy of 50% [6]. Finally, the size of the CP-violating nucleon-nucleon interactions has been calculated in terms of the chromo-EDMs of the quarks with an uncertainty of only 20% [4]. Based on the existing calculations, the limits on fundamental CP-violating effects set by the Hg EDM experiment are comparable to or better than the limits set by the experiments searching for a permanent EDM of an electron [8] or a neutron [9]. Thus, improvements in the atomic and nuclear theory of ^{199}Hg will better define the range of CP-violating parameters allowed by present and future experimental limits.

While the atomic theory of the Hg atom is more complicated than that of alkali-metal atoms because of the presence of two relatively loosely bound $6s$ electrons, it can be improved by including the correlation effects, which were not calculated in [6]. Our measurement of the Stark shift, combined with existing results for the oscillator strengths and the hyperfine structure of Hg, can be used for verification of the atomic calculations. The second motivation for our measurement is to provide a convenient diagnostic of the electric field in the on-going effort to improve the experimental limit on the EDM of ^{199}Hg.

Most previous experiments with Hg atoms, including measurements of the hyperfine structure [10] and the tensor Stark polarizability of the $6\,^3P_1$ state [11,12], have been done using resonance lamps as a light source. A narrow-bandwidth laser at 254 nm was recently built in our laboratory, allowing much more accurate measurements of Hg atomic properties. We believe that this is the first precision measurement of the Stark shift of a UV transition frequency.

Most Stark shift experiments have used an acousto-optic modulator (AOM) to calibrate the frequency shift. We chose to use a simpler method relying on the Doppler shift of the light reflected from a moving mirror. The frequency calibration was performed using a mechanical system to move a retroreflector with a known velocity. Additional checks were done by analyzing in detail Hg absorption profiles and using known hyperfine structure and the Doppler width of the resonance lines.

The Stark shift of an atomic state can, in general, be separated into scalar and tensor components [11]. For a state with a hyperfine structure ($\vec{F}=\vec{J}+\vec{I}$) the Stark shift is given by [13]

$$W(F,m_F) = -\frac{1}{2}\alpha_0 E^2 - \alpha_2 \frac{[3m_F^2 - F(F+1)][3X(X-1) - 4F(F+1)J(J+1)](3E_z^2 - E^2)}{(2F+3)(2F+2)2F(2F-1)2J(2J-1)}, \quad (1)$$

where $X = F(F+1) + J(J+1) - I(I+1)$ and E_z is the projection of the electric field $\vec{E}$ onto the spin quantization axis defined by the magnetic field. Here α_0 and α_2 are the scalar and the tensor polarizabilities, respectively. In ^{199}Hg the ground $6\,^1S_0$ state has $J=0$ and $I=1/2$. Therefore, the tensor polarizability vanishes. The excited $6\,^3P_1$ state of Hg has $J=1$ and a finite tensor polarizability α_2, which has been measured in [12] with an accuracy of 1%. However, the $F=1/2$ hyperfine component of the $6\,^3P_1$ state does not shift due to the tensor polarizability. Therefore, for the transition

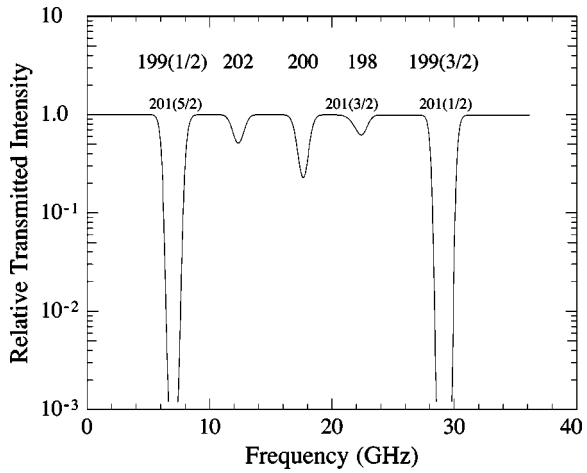

FIG. 1. Transmission through the cell containing room-temperature vapor pressure of isotopically enriched ^{199}Hg. A fit to the data gives the following abundances of Hg isotopes: ^{199}Hg 92%, ^{200}Hg 4.0%, ^{202}Hg 1.8%, ^{198}Hg 1.1%, and ^{201}Hg 1.1%. Hyperfine components of the lines are shown in parentheses.

$6\,^1S_0 \rightarrow 6\,^3P_1(F=1/2)$ the Stark shift is given by

$$W(6^3P_1) - W(6^1S_0) = -\tfrac{1}{2}[\alpha_0(6^3P_1) - \alpha_0(6^1S_0)]E^2. \tag{2}$$

The shift is independent of the direction of the electric field and the spin polarization of the atoms, which is convenient for *in situ* measurements of the electric field in the EDM experiment.

II. MEASUREMENT TECHNIQUE

The measurements were done using Hg cells containing room-temperature vapor pressure of isotopically enriched ^{199}Hg. In the absence of a buffer gas the absorption lines are optically thick, as shown in Fig. 1. High frequency sensitivity can be obtained by tuning the laser to the side of ^{199}Hg resonances and monitoring the transmitted intensity.

The cells are fabricated from Suprasil quartz tubing and disks. To apply a well-defined electric field we chemically coat the inner surfaces of the disks with a thin conductive and transparent film of SnO before assembly. The disks are glued to the body of the cell using TorrSeal epoxy. For the cell used in most measurements the distance between the inner surfaces of the disks is (11.33 ± 0.07) mm. The cells are evacuated and baked out at 120 °C. ^{199}Hg vapor is admitted into the cells until a visible film condenses inside. High voltage up to 10 kV can be applied between the disks without breakdown. The high voltage was measured with 0.2% accuracy.

The laser light at 254 nm is produced by frequency quadrupling the output of a single-frequency semiconductor laser to achieve low amplitude noise and long term stability. A schematic of the laser is shown in Fig. 2. The MOPA (master oscillator-power amplifier) system was manufactured by SDL. Enhancement cavities are built around each of the nonlinear crystals to increase the efficiency of second-harmonic

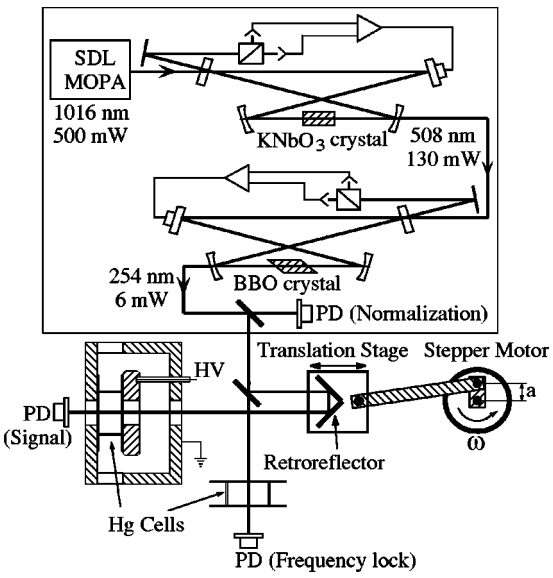

FIG. 2. A simplified schematic of the UV laser and the setup for Stark shift measurements. A calibrated freqeuncy shift is created by a moving retroreflector.

generation. The second cavity uses superpolished mirrors with a dielectric coating made using ion-assisted deposition. The cavities are locked to resonance using the Hänsch-Couillaud scheme [14]. The output power of the laser is 6 mW. By using acoustical isolation the intensity noise is reduced to $10^{-4}/\sqrt{\text{Hz}}$. A more detailed description of a similar laser operating at 243 nm can be found in [15].

The amplitude noise is further reduced by a feedback system adjusting the current of the power amplifier to keep the intensity constant. Furthermore, the outputs of the signal and the frequency lock photodiodes are divided by the output of the normalization photodiode using analog dividers before being recorded by the computer. The frequency of the laser is locked to the side of the ^{199}Hg resonance by adjusting the current in the master oscillator to keep the transmission through a Hg reference cell constant.

Most of the measurements were done with the laser beam going through the electric plates as indicated in Fig. 2. The changes in the transmitted intensity as the electric field is turned on and off are shown in Fig. 3. By averaging several such scans the statistical uncertainty is reduced to 1%.

To determine the absolute size of the Stark shift it is also necessary to measure the slope of the transmission curve in units of frequency. This was done by applying a known Doppler frequency modulation created by an oscillating retroreflector and measuring the resulting change in transmission. The Doppler frequency shift is given by

$$\Delta\nu = \nu_0 \frac{2v}{c} = \frac{2\nu_0 \omega a}{c}, \tag{3}$$

where $\nu_0 = 1.182 \times 10^{15}$ Hz is the resonance frequency of the Hg transition, ω is the angular rotation frequency of the stepper motor, and $a = (0.250 \pm 0.002)''$ is the amplitude of the motion. In making this measurement it was important to re-

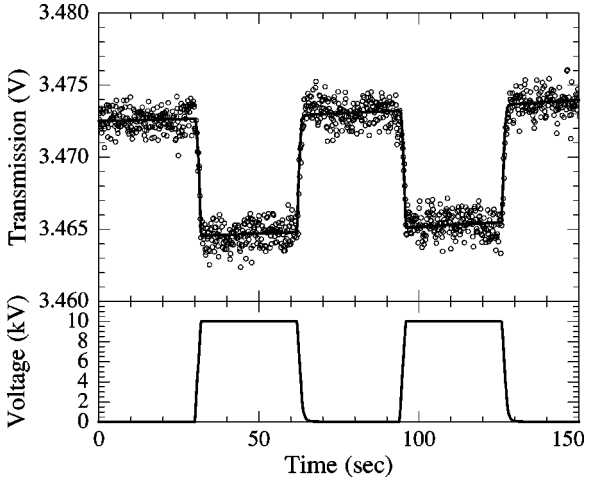

FIG. 3. Change in the transmission of the laser (top panel) tuned to the side of the ^{199}Hg resonance as the high voltage (bottom panel) is turned on and off. The fit of the data (solid line) includes a term proportional to V^2, as well as a linear and quadratic drift.

duce a spurious signal due to the motion of the laser beam. This background can be measured by detuning the laser off resonance. By careful laser alignment the background could be reduced to less than 10% of the Doppler signal. It was further reduced by using the fact that it depends on the position, not the velocity of the retroreflector. Oscillations in the transmitted intensity in phase with the velocity of the retroreflector were recorded by a lock-in amplifier. Furthermore, the measurements were done at several rotation frequencies ω, from $2\pi\times 2$ Hz to $2\pi\times 8$ Hz. The lock-in signal as a function of the rotation frequency is shown in Fig. 4. A linear fit to these data was used to calculate the slope of the transmission curve at a given laser wavelength. We estimate that the systematic error was less than 0.9% by checking for a nonlinearity of the lock-in signal.

Independent measurements of the slope were performed by analyzing a wide frequency scan shown in Fig. 1. The

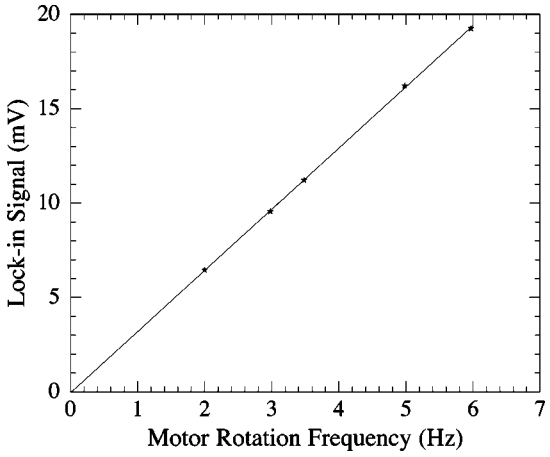

FIG. 4. Frequency calibration using the Doppler shift from an oscillating mirror. The lock-in signal measures the amplitude of the intensity oscillations in-phase with the velocity of the mirror. A linear fit to the data (solid line) is used to calculate the slope of the transmission curve.

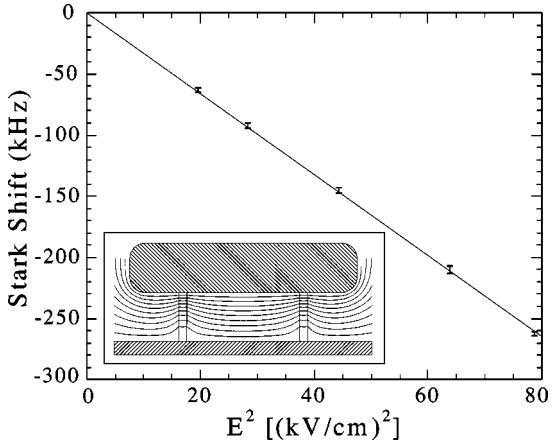

FIG. 5. The Stark shift as a function of E^2. From the linear fit to the data (solid line) the Stark shift is (-3.331 ± 0.016) kHz/(kV/cm)^2. Errors are statistical and $\chi^2/ndf=1.0$. The inset shows a calculation of the electric equipotential lines inside the cell for a nonuniform voltage drop on the walls and assuming cylindrical symmetry.

frequency axis of the scan was determined by fitting the data to a series of Gaussians with the hyperfine structure and the Gaussian width held fixed. The fit was used to calculate the slope of the transmission curve as a function of the relative transmitted intensity with an error of about 1%. The two methods of determining the slope agreed within 1%. We also compared the two techniques on the sides of the ^{200}Hg resonance, which has much smaller optical thickness.

III. RESULTS AND ESTIMATES OF SYSTEMATIC EFFECTS

The results of the Stark shift measurements as a function of the electric field are shown in Fig. 5. All results for high voltage of 10 kV are shown in Fig. 6. For these measurements the magnetic field was perpendicular to the electric field and the laser was linearly polarized parallel to the magnetic field. The measurements were performed at different

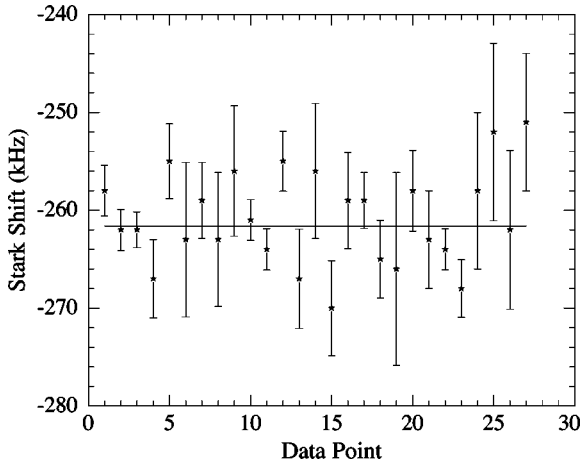

FIG. 6. All measurements performed at $E=8.875$ kV/cm under a variety of conditions. The average shift is (-261.6 ± 0.6) kHz. The errors are statistical, $\chi^2/ndf=1.3$.

frequencies on both sides of the $F=1/2$ resonance, with transmission ranging from 10% to 80%. Approximately equal numbers of measurements were taken on each side. The high voltage dwell time was varied from 5 to 30 sec. The intensity of the laser was varied from 7 to 20 μW/mm^2, while the saturation intensity is 330 μW/mm^2. No systematic effects were observed. The χ^2/ndf is equal to 1.3 for all measurements at 10 kV.

Electric-field nonuniformity inside glass cells is a possible source of large systematic effects. As was found by Hunter and co-workers [13], the voltage drop across an uncoated glass surface is not uniform. This problem was largely avoided by directing the laser beam through the electrodes, so that the integral of E along the path of the beam is fixed by the applied voltage. However, a higher-order effect remains, since the Stark shift is proportional to the integral of E^2 along the path of the beam. The electric field inside the cell was studied in more detail by sending the laser beam parallel to the electrodes, through additional windows shown in Fig. 2. It was found that when the laser beam was close to one of the electrodes, the Stark shift depended on the polarity of the applied high voltage and was always stronger near the negative electrode, in agreement with [13]. In the worst case the Stark shift was different by a factor of 3 between the two polarities. To estimate the size of the correction for the laser beam directed perpendicular to the electrodes we used an electrostatic simulation program [16]. We calculated the electric field inside the cell for a nonlinear voltage drop along the glass wall, assuming cylindrical symmetry. A typical result is shown in the inset of Fig. 5. As expected, the electric field is substantially more uniform near the center of the cell. The integral of E^2 was calculated along various lines through the cell and compared with measurements to validate the model. For the laser beam directed along the axis of the cell the average value of E^2 is increased by $0.7\pm0.4\%$ due to field nonuniformity. If the laser beam is displaced by 5 mm from the axis, the Stark shift increases by an additional 1%.

The tensor Stark shift, which does not contribute directly to the shift of the $F=1/2$ resonance in ^{199}Hg, introduces two small systematic effects. The first is due to isotopic impurities in our ^{199}Hg sample. The ^{199}Hg $F=1/2$ resonance line overlaps ^{204}Hg and ^{201}Hg ($F=5/2$) lines, which have a tensor Stark shift. The ^{201}Hg ($F=5/2$) line, in particular, produces an apparent tensor shift on the high-frequency side of the ^{199}Hg $F=1/2$ line. Using isotopic abundances determined from data shown in Fig. 1 and the tensor polarizability of the $^3P_1$ state [12], we calculate that the systematic error due to the presence of ^{201}Hg is less than 0.4%.

The other effect of the tensor shift is to produce a small mixing of $F=1/2$ and $F=3/2$ levels in ^{199}Hg [13]. This mixing causes a change in the relative strength of the two hyperfine lines. Since we are relying on a change in the transmitted intensity to measure the frequency shift, it will cause a systematic effect. However, the effect has opposite signs on the two sides of the resonance and is eliminated by making measurements on both sides. We calculated that it should produce a 0.8% difference between the Stark shifts measured on the two sides of the $F=1/2$ resonance, which is less than the error of our measurements.

We also checked the size of the tensor shifts by making measurements with the magnetic field parallel to the electric field. The spin quantization axis used in Eq. (1) is defined by the magnetic field, since the Zeeman interaction in the 6^3P_1 state for our field of 30 G is much larger than the Stark shift. The tensor shifts are proportional to the term $(3E_z^2-E^2)$ which changes from $-E^2$ to $2E^2$ when the angle between the magnetic and electric fields is changed from $\pi/2$ to 0. The measured Stark shift changed by about 1%, in agreement with the estimates above.

Including the 0.7% correction for the nonuniformity of the electric field, our final result for the scalar Stark shift of the $6\,^1S_0\rightarrow 6\,^3P_1$ transition frequency is -3.32 ± 0.06 kHz/(kV/cm)^2. The error is dominated by systematic uncertainties, mainly electric plate spacing (1.2%), the slope measurements (1.2%), and the contribution of the tensor Stark shift (0.5%). From this result the difference between the scalar polarizabilities of the $6\,^1S_0$ and $6\,^3P_1$ states is $\alpha_0(^3P_1)-\alpha_0(^1S_0)=(3.95\pm0.07)\times10^{-24}\,\mathrm{cm}^3$.

We also performed a study of the electric field in the cells used for the EDM experiment. The cells contain 500 Torr of N_2 and 50 Torr of CO gas. Pressure broadening of the absorption lines reduces the slope of the transmission curve, making the measurements noisier. The cells have a paraffin $[CH_3(CH_2)_{30}CH_3]$ coating on the inside walls, which dramatically improves the uniformity of the electric field. With the laser beam near one of the electrodes, the Stark shift changed with polarity of high voltage by less than 3%. By averaging several hundred scans we measured the Stark shift in an EDM cell to be -3.34 ± 0.04 (stat. only) kHz/(kV/cm)^2, in very good agreement with our other result.

In conclusion, we have made the first measurement of the scalar Stark shift of the $6\,^1S_0\rightarrow 6\,^3P_1$ transition in ^{199}Hg. The measurement can be used as a check for an improved calculation of the Hg atomic wave functions. Such calculation would reduce the uncertainty in the interpretation of the limit on the EDM of ^{199}Hg. We also established that the electric field in the cells used in the new EDM search is uniform and reversible.

ACKNOWLEDGMENTS

We would like to thank M. Chasan for running the electric-field simulation program. This work was supported by the NSF through Grant No. PHY-9732513.

[1] L.R. Hunter, D. Krause, Jr., D.J. Berkeland, and M.G. Boshier, Phys. Rev. A **44**, 6140 (1991).

[2] C.E. Tanner and C. Wieman, Phys. Rev. A **38**, 162 (1991).

[3] J.P. Jacobs, W.M. Klipstein, S.K. Lamoreaux, B.R. Heckel, and E.N. Fortson, Phys. Rev. A **52**, 3521 (1995).

[4] T. Falk, K.A. Olive, M. Pospelov, and R. Roiban, Nucl. Phys. B **560**, 3 (1999).

[5] V.V. Flambaum, I.B. Khriplovich, and O.P. Sushkov, Phys.

Lett. **162B**, 213 (1985).
[6] A.M. Martensson-Pendrill, Phys. Rev. Lett. **54**, 1153 (1995).
[7] J. Engel, J.L. Friar, A.C. Hayes, Phys. Rev. C **61**, 035502 (2000).
[8] E.D. Commins, S.B. Ross, D. DeMille, and B.C. Regan, Phys. Rev. A **50**, 2960 (1994).
[9] P.G. Harris *et al.*, Phys. Rev. Lett. **82**, 904 (1999).
[10] I. M. Popescu and L.N. Novikov, Compt. Rend. **259**, 1321 (1964).
[11] A. Khadjavi, A. Lurio, and W. Happer, Phys. Rev. A **167**, 128 (1968).
[12] R.D. Kaul and W.S. Latshaw, J. Opt. Soc. Am. **62**, 615 (1972).
[13] L.R. Hunter, D. Krause, Jr, S. Murthy, and T.W. Sung, Phys. Rev. A **37**, 3283 (1988).
[14] T.W. Hänsch and B. Couillaud, Opt. Commun. **35**, 441 (1980).
[15] J. Torgerson and W. Nagourney (unpublished).
[16] Maxwell 2D Field Simulator from Ansoft Corp., www.ansoft.com.